Mandibular cortical width measurement based on dental panoramic radiographs with computer-aided system

***Przemysław Maćkowiak, **Tomasz Kulczyk, ***Elżbieta Kaczmarek**

*Faculty of Electronics and Telecommunications
University of Medical Sciences
Poznań University of Technology, Poland

**Department of Biomaterials and Experimental Dentistry
University of Medical Sciences
Poznań University of Technology, Poland

***Department of Bioinformatics and Computational Biology
University of Medical Sciences,
Poznań University of Technology, Poland

***Abstract*—The paper presents a method of the determining a mandibular cortical width on dental panoramic radiographs. Cortical width of lower border of mandible may potentially be associated with recognition of osteoporosis in postmenopausal women. An algorithm to perform a semiautomatic cortical width measurement in a given region of interest was developed. The algorithm is based on separate extraction of lower and upper boundaries of cortical bone. Results of boundaries extraction performed on 34 panoramic radiographs of healthy and osteoporotic individuals are presented, together with automatic measurements of particular distances. They were compared with results of hand-made measurements done by two maxillofacial radiologists. Presented algorithm may potentially be useful for screening patients with osteoporosis.**

***Index Terms*— dental panoramic tomogram, dentistry, edges extraction, osteoporosis, segmentation.**

I. INTRODUCTION

Osteoporosis is characterized by low bone mass density and deterioration of microarchitecture of bone. This disease is resulting in increased skeletal fragility and fracture susceptibility and is recognized as one of causes of morbidity and mortality in postmenopausal women [1]. Low bone mass density (BMD) can be diagnosed by means of densitometric techniques such as double-energy X-ray absorptiometry (DEXA) method performed in the region L1-L4 of spinal column or a hip. This method is very precise however is rather expensive, requires some fine equipment usually located in specialized medical centers and cannot be performed on large population group. Therefore many authors suggest that some other potentially cheaper and more accessible methods of recognition of disease should also be developed. These methods may not necessarily be used to make a full diagnosis of the osteoporosis but to be helpful for screening of larger populations. One of proposed method is based on estimation of some parameters of mandible. Correlations between low parameters of mandibular BMD and the BMD of the spinal column and hip have been found in some studies [2],[3]. Also a densitometry of the mandible has been done by some of the authors but this method is restricted to be used in edentulous patients only [4]. Dental panoramic images are used extensively in dental practices all over the world. The sample image was shown in Fig. 1A.On these radiographs some anatomical and pathological structures can be found and information provided by panoramic images are helpful to establish a proper diagnosis, to propose a treatment plan and to evaluate the results of the treatment. Panoramic radiograph provides an excellent image of mandible with clear details of cortical bone and as truly cheap and easily available method for the large population should be considered one potentially useful for screening of osteoporosis A number of studies in this field use panoramic X-rays for the estimation of different mandibular parameters [5].These are mainly the distances between particular elements on the body of mandible. As a result thickness of cortical part of the bone (so called cortical width) can be

.

established. Some authors conclude that if the cortical width is less than 3mm, an individual should be referred to seek further osteoporosis investigation [8].

Currently used methods of measurement involve making a number of linear drawings on panoramic image which are used to identify the mandibular cortical bone. After identification manual measurements of distances between points of interest are done by a radiologist. This method is time consuming as it is performed manually by the radiologist by means of ruler and a pen.

The purpose of this paper is to present the method for measuring the cortical width which does not need the training data and can be performed quickly.

II. REVIEW OF OTHER WORKS

There are only a few algorithms that were designed for mandibular cortical width measurement on dental panoramic radiographs. One of them is based on the active shape models using training data [6]. The core is PDM (Point Distribution Model), which requires to manually point the landmarks. The second algorithm [7] measures the parameter in the region of the mental foramen. Unfortunately, it needs manual assistance after region of interest was determined. The former is described at the beginning and the later at the end of the present section.

Some scientists concluded that the cortical width on a dental panoramic radiograph can be helpful in osteoporosis investigation, which is characterizes by low BMD level. Arifin et al [7], [10] worked on computer-aided system for measuring above parameter. The authors stated that them program can be useful for identifying postmenopausal women with low skeletal BMD level. Their algorithm is not fully automatic unfortunately. The following steps were performed by them: region of interest determination, image enhancement, cortical margin identification, distance measurement. The algorithm is described more precisely below.

The first step is to define the region of interest. The reason is to decrease the computation time and to prepare an image to further processing. An operator has to find the mental foramen which is the landmark point. A rectangular area around it is the region of interest. It includes both the mandibular and the trabecular bone. The next step is to distinguish the mandibular bone from other objects. First, the background is eliminated. The highpass filtering is used to emphasize the high brightness variation. An image is thresholded, the smallest values are assigned as black color, others as white color. Then, the opening and closing operations are used. The tracing algorithm and compression steps are used to extract the lower and upper mandibular bone boundary. The former needs two starting point which are associated with the boundaries. They are pointed by an examiner. Then, the contours of the outer and inner margin are found. These curves are the input to the compression step. It removes unnecessary points, which can noised the measurement. The measurement requires two points. One of them belongs to the outer margin and one belongs to the inner margin. The cortical width is the Euclidian distance between them. The selection of the appropriate points is following. The regression lines are drawn through each point belonging to the outer margin. The construction is based on some number of neighborhood points. The gradient of regression line is associated with each point of the outer margin. A point for which the perpendicular line to the regression line passes the mental foramen is selected. The second point is the intersection point between the inner margin and the perpendicular line to the regression line at the outer margin point selected previously. As was mentioned above, the cortical width is Euclidian distance between two points found.

The authors do not give deep explanation about the parameter “number of tracing point”, which controls the tracing algorithm. They do not consider the size of the structural elements used for morphological operations. They do not analyze the size and the values of the mask used in highpass filtering neither.

The margins can be detected wrongly when undesired structures (e.g. the hyoid bone) are presence on the region of interest. The algorithm is not robustness for such situation.

The second algorithm is based on statistical shape models. The patient data consist of 132 dental panoramic radiographs. The algorithm requires the training data. Main core of active shape models is PDM. Two examiners put the set of points (the landmark points), which represent the mandibular margins. 50 equally spaced points were put along the mandibular margins between the ante-gonion and the mental foramen on each image side. PDM contains information on the principle modes of landmark points variations. The mandibular shape for each of training set is described by the coordinates of all landmark points. Let vector $x = (x_1,y_1,x_2,y_2,x_3,y_3,...,x_n,y_n)$ be the set of these coordinates, where n is the number of points. New shape can be approximated by following equation: $x = \bar{x} + Pb$, where $\bar{x}$ is the mean shape, P is the matrix containing the eigenvectors of the covariance matrix and b is a vector of weights associated with the eigenvectors. The authors tested the algorithm on examples witch were not included in the training set.

III. BOUNDARIES EXTRACTION

Dental panoramic radiograph contains low-contrast structures. The edge detection is not a simple task for that reason. Additional difficulties arise due to noise. The mandibular bone is restricted by the upper and lower boundary. The lower boundary is in the higher contrast region than the upper boundary. The contrast along the boundary is not solid. One of the main reasons is that the bone contains different amounts of the calcium.

The input image was a part of dental panoramic radiograph which was cut by the radiologist in relation to the mental foramen and the lower mandibular bone margin. They contain the mandibular bone and the region below the lower cortical bone boundary. The mental foramen is either in the left upper or in the right upper corner of the image. The sample region of interest was shown in Fig. 1B. Fig. 1A presents the complete dental panoramic radiograph (there are two regions of interest).

A. Lower boundary extraction

Edges can be detected using Sobel, Roberts or Prewitt kernels. This approach is not appropriate in this application. The problem is the mask size and proper thresholds setting, which follow the edges map. Thanks to that, the edges are often broken and the underlying mechanism does not ensure the extraction of the one edge only, which corresponds to the lower boundary of the mandibular bone. The Laplacian of Gaussian (LoG) method and zero-cross searching seems to be a better approach. The algorithm does not ensure the continuity of the lower boundary either. The problem arises with the choice of the appropriate standard deviation value of the LoG filter. The similar situation is in the Canny algorithm. The discontinuity takes place where the contrast in the lower boundary region is not explicitly uniform. The settings of thresholds are crucial and their experimental choosing for each image is time consuming.

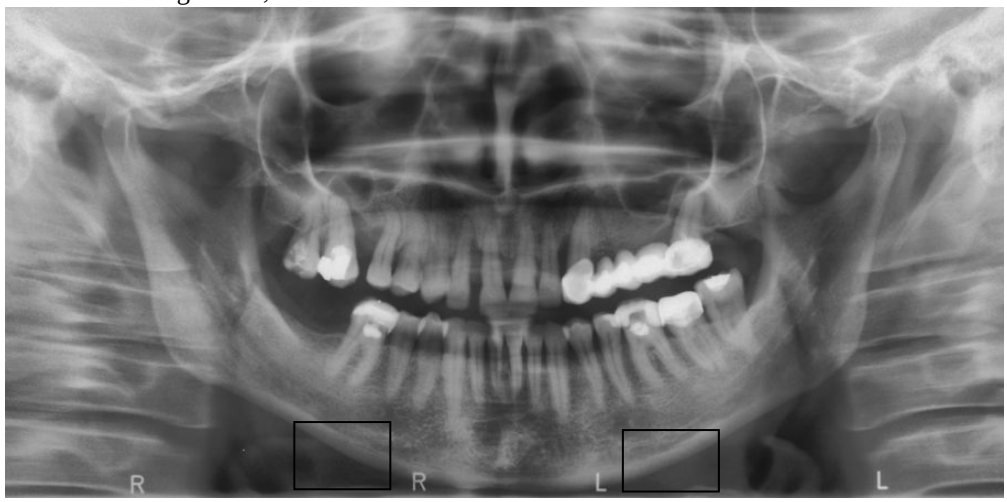

A

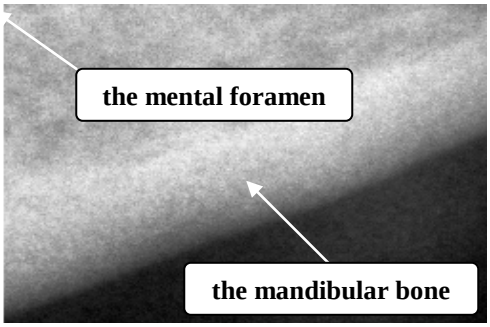

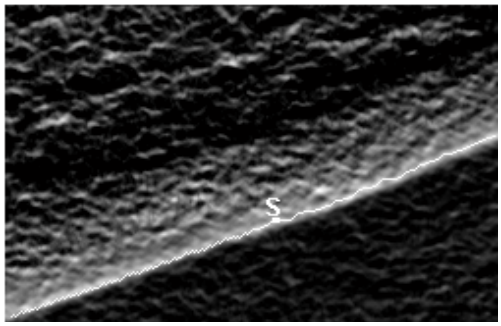

B C

Fig. 1. A – the panoramic radiograph with two black rectangulars pointing at the region of interest. B – the region of interest showing the mandibular bone fragment. C – the image gradient, S corresponds to the starting point, the white path is the lower mandibular bone boundary.

Due to mentioned reasons the lower boundary extraction algorithm is presented below. It generates single edge only what is its advantage over the mentioned methods. Its description is divided into two parts. The first part depends on an image gradient computing. The second stage is determining path that corresponds with the lower boundary.

1) Image gradient

The following steps are carried out for each input image pixel.

a) i=1, N=3.
b) Compute directional derivative for 45°, 90° and 135° using NxN kernel in each case.

c) Compute G_i as the sum of two highest value of the three directional derivatives computed in the previous step, i=i+1.
d) Change N value for higher value to increase the kernel size (for example N=N+2) and go to step b), otherwise go to step e).
e) The output value of the pixel of interest is the highest value of set $\{G_i\}$.

The three directional derivatives are computed in step b). Their choice is the result of the spatial orientation of the lower mandibular bone boundary in the region of interest (the highest values of gradient are for derivatives computed for the angle equals to either 45° or 90° on the right side image, and for derivatives computed for the angles equals to 90° or 135° on the left side). To adjust the kernel size to the spatial edge size, the output value is max(G_i) [9]. The example of original and output image are shown in Fig. 1B and 1C respectively. Fig. 2 presents the block diagram which describes the image gradient computing. $G_1$45, $G_1$90, $G_1$135 are blocks which compute the directional derivative for the angles 45°, 90° and 135° respectively. The higher i index the greater mask. MAX SUM block sums the two greatest values. MAX block selects the greatest value. The three dimensional plot as a function of position of two variables presents an image of the mountains and valleys. The pixels which lie along the lower boundary have high brightness value. Their position corresponds to the mountain region.

2) Path determination

The second stage of the algorithm is "walking in the mountains". It is responsible for determining the path, which corresponds with the lower mandibular bone boundary. It consists of the following steps.

a) Determine the weights associated with areas A, B, C, D, E, F depending on image side. Select a starting point.
b) Determine the first direction search (either the east or the west direction).
c) According to the starting point, compute sums of brightness in each region A, B, C for the west direction or in the regions D, E, F for the east direction (see Fig. 4).
d) Multiply the values received by the appropriate weights (see Table 1).
e) Mark the pixel which is associated with the highest multiplication result. The marked pixel becomes the new starting point.
f) Jump to step c) if the image boundary (first or last column) is not reached, otherwise go to step g).
g) Go to step h) if the second direction search is not started, otherwise stop the algorithm.
h) Determine the second direction searching in the opposite direction to that used in step b). Set the starting point to the one, which was determined in step a) then jump to step c).

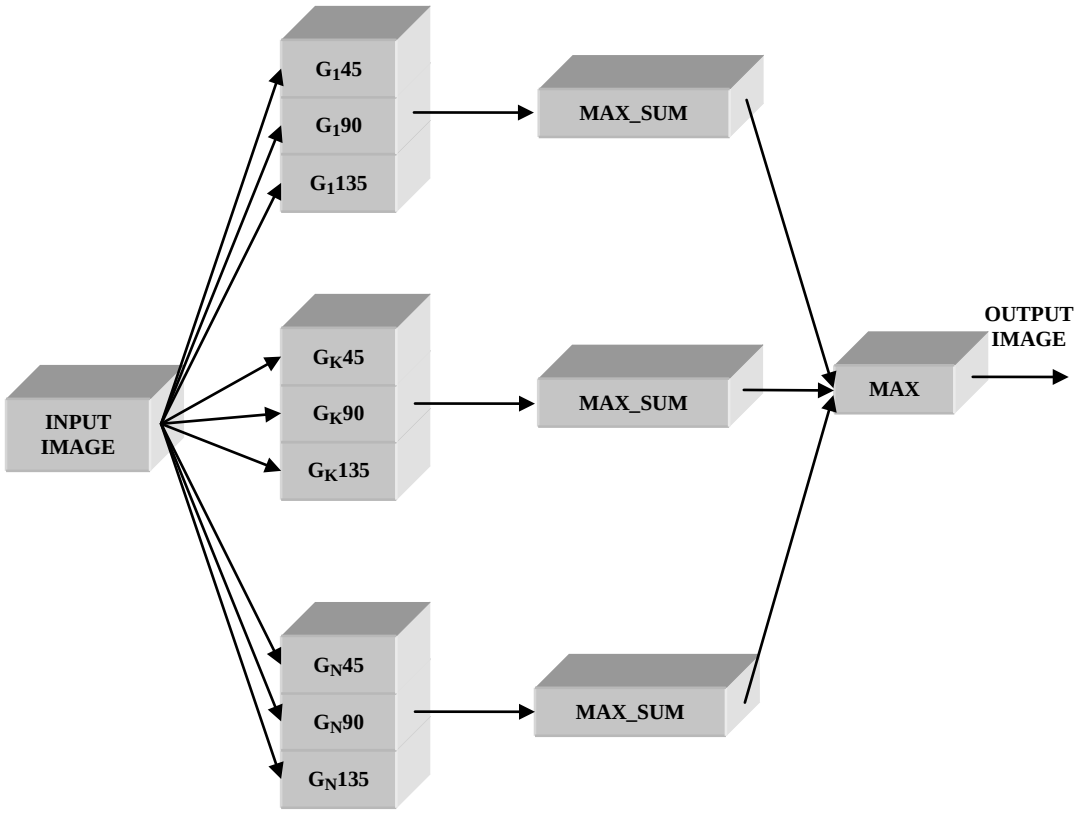

Fig. 2. The block diagram of the gradient computing procedure.

The set of pixel marked create the lower boundary. The starting point is selected based on the image gradient. It is located in the lower boundary region (the mountain region). The path which corresponds to the lower boundary follows the brightness regions. The starting point can be determined manually (an expert points its appropriate location on the image) or automatically. The simple algorithm of the automatic starting point determination is presented below.

a) Threshold the image gradient using 90th percentile level as the cutoff threshold.
b) Leave the object whose area is the greatest.
c) The starting point is the middle point of the lower boundary object received.
d) Perform the starting point location correction, moving the pixel vertically to the nearest brightness maximum.

Then, the starting point should lie on the mountain region.

A - F are the regions containing nine pixels. Some of them overlap (like A and C or D and E). The intensity sum of region F is the sum of intensities creating region F. The intensity sums are computed in regions A, B, C (when the path determination is carried out west) or in regions D, E, F (when the path determination is carried out east). The numbers received are multiplied by the expert weights defined (weights are selected to favor some direction search, where the pixels creating boundary should lie). The region associated with the highest value is selected. The boundary pixel is pixel N1 when region A is selected.

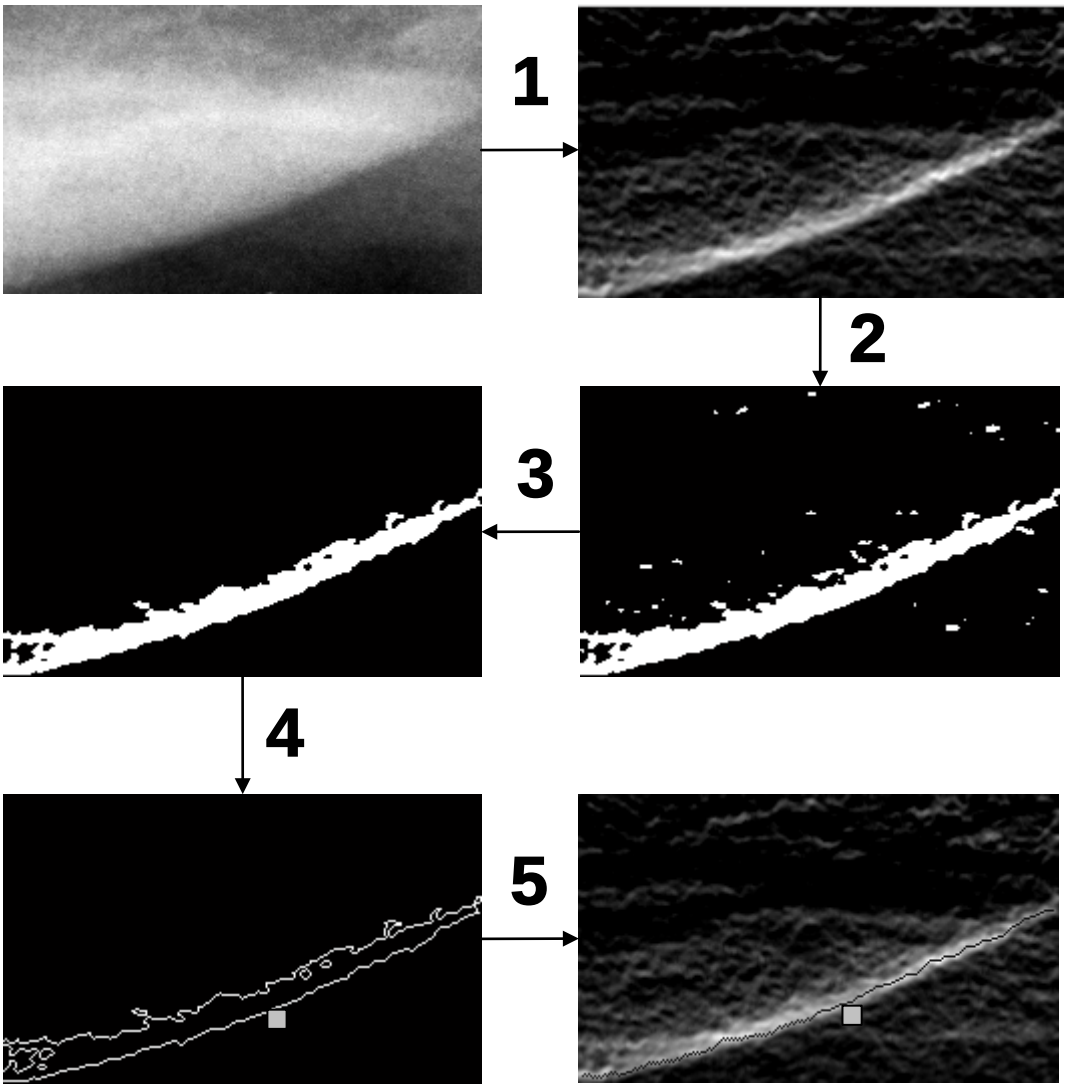

Fig. 3. Determination of the lower cortical margin.

pixel N3 when region B is selected, N5 when region C is selected, pixel N2 when region D is selected, pixel N4 when region E is selected, region N6 when region F is selected. The pixel selected is the new starting point.

TABLE 1. THE EXAMPLE WEIGHTS ASSIGNED TO THE REGIONS. *- FOR LEFT IMAGE SIDE, **- FOR RIGHT IMAGE SIDE

Region	A	B	C	D	E	F
Weights*	1.0	1.0	1.5	1.5	1.5	1.0
Weights**	1.5	1.5	1.0	1.0	1.0	1.5

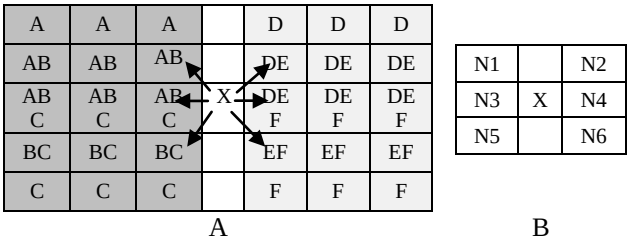

Fig. 4. A – regions where the intensity sums are computed. X is the pixel of interest. B – the matrix of the neighbors of pixel X.

The different weights are used depending on image side. This means that an expert should sort the images into two categories: left side images and right side images.

B. Upper boundary extraction

The upper boundary lies in the low contrast region. This is the fundamental difficulty in its extraction. The algorithm is divided into two parts. The first is that of the maximums estimation. First brightness maximum lies usually in the region of the upper boundary. The second stage is the estimation of the inflection points. The inflection points are at places where rapid intensity changes exist. They correspond to the points which belong to the upper bone boundary.

1) Maximums estimation

To begin with the lower boundary is extracted. Specific points are selected on the lower boundary extracted (for example every 4-th pixel). Next, the profiles are drawn. The profile is the function of brightness depending on the location. The set of profiles is $\{s_j[k]\}_j$, j=1,2,…n, where n determines the total number of points selected. The profile is the perpendicular line to the tangent to the lower cortical bone boundary at the specific point. The method is described by two parameters m, p. The former points at maximums number, the later at difference. MAX_PROFILE is the table which contains the first maximums of the profiles denoised. MAX is the table which contains the maximums estimated.

a) Let j=1, $\sigma=\{1.0,1.5,2.0,2.5,3.0,3.5,4.0,4.5\}_i$.
b) Let i=1.
c) Filter profile $s_j[k]$ using two dimensional Gaussian filter (standard deviation equals σ_i).
d) Find the location of the first brightness maximum of the denoised profile, store it in MAX_PROFILE(i,j), i=i+1.
e) Go to step c) if i<9, otherwise go to f).
f) Locate j-th column in MAX_PROFILE table, and find the first m-elements series whose elements do not differ by more than p. The estimated maximum is the value of the first series element, store it in MAX(j).
g) Go to step a) if j≤n stop algorithm, otherwise stop the algorithm.

2) Inflection points estimation

The upper boundary points are located at the region where the rapid intensity changes exist. Therefore, the infection points are estimated. The estimated maximums can be noisy, therefore a correction of their location may be needed using the median filtering. MAX_UPDATE is the table which contains the corrected maximums. med(MAX) and med(OUT) determines the median filtering of the signal MAX and OUT. The filtered signals are denoted by m1 and m2 respectively. INDEX is helpful table whose elements contain the indices associated with the maximums corrected. INF is the table which contains the inflection points. The locations of the points which belong to the upper boundary, are located in the table OUT.

a) Let j=1.
b) Let m1 = med(MAX),
c) Find the element in the j-th column of MAX_PROFILE which is the nearest to m1(j) and store it in MAX_UPDATE(j), store its row index in INDEX(j).
d) Filter profile $s_j[k]$ using the two dimensional gaussian function (standard deviation equals $\sigma_{INDEX(j)}$).
e) Find the location of the first inflection point after MAX_UPDATE(j) of the denoised profile and store it in INF(j), j=j+1.
f) Go to step c) if j≤n, otherwise let j=1 and go to point g.
g) Let m2 = med(INF).
h) Find the location of the nearest inflection point to m2(j) and store it in OUT(j), j=j+1.
i) o to point h) if j≤n, otherwise stop the algorithm.

The infection points estimated are the points which create the upper boundary. The corrected maximums and the inflection points estimated were shown in Fig. 5 and Fig. 6 as black bars (for m=3, p=5).

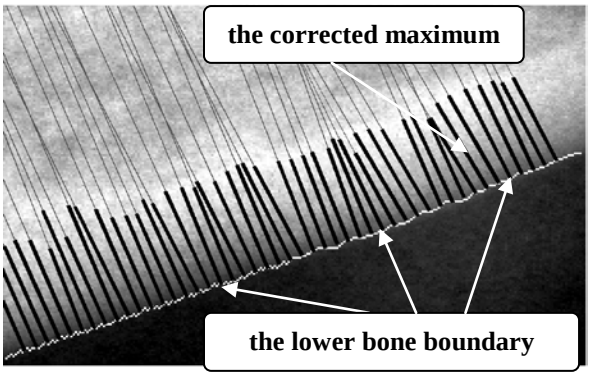

Fig. 5. The corrected locations of the maximums.

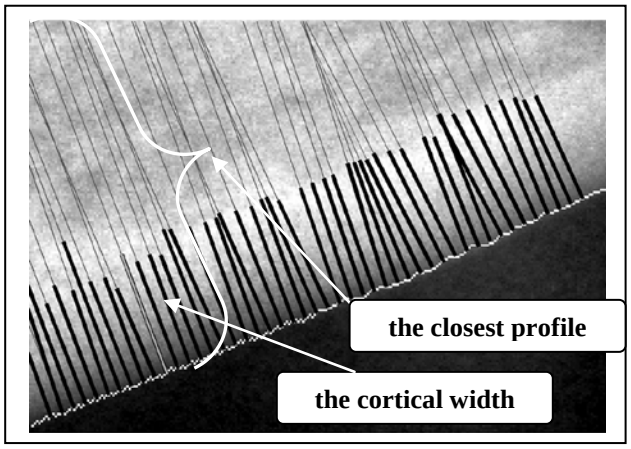

Fig. 6. The inflection points estimated.

IV. EXPERIMENT AND RESULTS

The upper and lower boundary extraction algorithms were tested on panoramic images. Thirty four dental panoramic radiographs were provided by the Section of Dental Radiology of xxxxxxxxxxxxxxx xxxxxxxxxxxxxxxxxxxxx University of xxxxxxxxx xxxxx. The digital images have been taken using the CRANEX TOME dental panoramic unit and a DIGORA PCT PSP DIGITAL SCANNER.

This set of unit/scanner utilizes a photostimulable phosphor plate (PSP) technology in which a weak radioactive signal is stored on a phosphor plate and later is released by stimulation with visible light, to produce a luminescent signal which can be seen and radiographic image. The resolution of panoramic images was 300dpi, which means that 1pixel corresponds to about 0.1mm. 68 regions of interest (ROI) at the region extending from mental foramen to below a lower cortical border of mandible were cropped from digital panoramic images to perform measurements and comparison. Each ROI was presented to two experienced radiologists to perform recognition of particular structures of mandible and to perform manually measurements of cortical widths. The same ROIs were also processed by the algorithms. The described algorithms were written in MATLAB 7.0.

The radiologist divided the images into noise free images (17) and cluttered images (17). The images were classified as cluttered if the region of interest contained structures which do not appear in a proper image. The cluttered images resulted from the improper patient head setting during the image acquisition process.

Next, the extraction of the lower and upper (for m=3, p=5) mandibular bone boundaries were performed. The radiologists drew the upper and lower boundary (the reference boundaries) for comparison. An area around the reference boundary was created using parameter d which determines the size of the area. The area is the set of pixels whose maximum distance (in the vertical direction) from the nearest point which create the reference boundary do not exceed d points. The area for different d was shown in Fig. 7. The total number of pixels received by the program which lies in the area is computed (the result is expressed in the percentages). The computations were carried out for the upper and lower boundary. The results were averaged for all images and were shown in Fig 8. The weights used in the lower boundary case, were the same as in Table 1. The boundaries extracted enable the measurement of the cortical width. It was carried out in the mental foramen vicinity. The measurement of cortical bone was carried out according to the approach below. A radiologist makes the tangent to the lower cortical bone boundary. The radiologist draws a second line that crosses the mental foramen and is perpendicular to the tangent. A measurement is carried out along the perpendicular line. The cortical width is the Euclidian distance between the two points which lie on the perpendicular line, one of which belongs to the lower boundary, whereas the second belongs to the upper boundary. From the set of profiles $\{s_j[k]\}_j$ the profile closest to the mental foramen is selected and a measurement along this profile is conducted. The profile crosses the lower and upper boundary at two points. The Euclidian distance between them is the cortical width. The gray segment in Fig. 6 corresponds to the cortical width. The radiologists measured the cortical width by hand. The program measured the cortical width according to the following steps.

a) Extract the lower cortical bone boundary.
b) Extract the upper cortical bone boundary.
c) Select appropriate profile
d) Compute the cortical width.

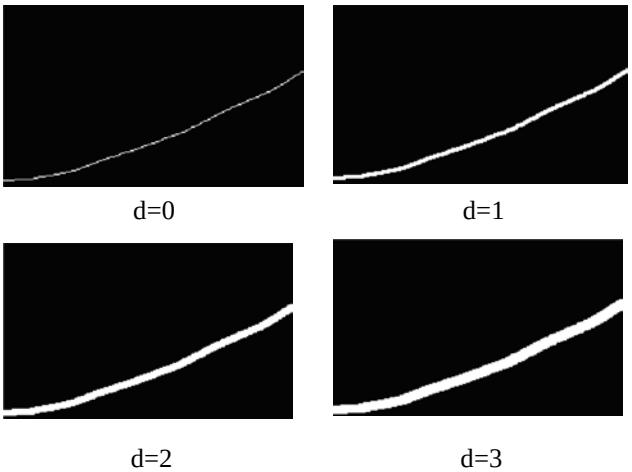

Fig. 7. An area around the reference boundary for d parameter equals 0, 1, 2 and 3 respectively.

Every forth pixel of the lower boundary was selected while the maximums estimation. The window span was 13 for the median filtering. A comparative analysis was done between the measurement of the cortical width took by program and the measurement of the cortical width took by the radiologists. The analysis took into account both the noise free images and the cluttered images. The results were presented by the Bland-Atman plot in Fig 9.

V. DISCUSSION

The one problem is the lack of the absolute "ground truth". Therefore, the measurements were done in comparison with measurement done by the radiologists. In this way, the results depend on the accuracy on the radiologist.

The estimation of maximums and inflection points is not proper for the cluttered images. In general, the estimation is not appropriate in the places, where the undesired structures exist. They distort the true shape of the mandibular. The lower boundary extraction algorithm selects the pixels associated with the highest intensity region. This is sometimes a problem for cluttered images, where the brightest region is not always associated with the next boundary pixel. The reason is the presence of the undesired structures (like the hyoid bone) which are a result of an improper acquisition process. In such a situation, the algorithm can lose the appropriate path and extract an improper edge.

VI. SUMMARY

The method for measuring the cortical width on dental panoramic radiographs was presented in the paper. It does not require any training data as in [6]. The extraction of the lower boundary requires the knowledge about which image side is processed. Involvement of the operator (like a dentist) is lass than in [7], [10]. The algorithm of the upper boundary extraction is not robust enough to precisely extract the upper boundary from cluttered images. In future investigation this problem should be solved.

The presented method may be useful for screening patients with osteoporosis based on the noise free images.

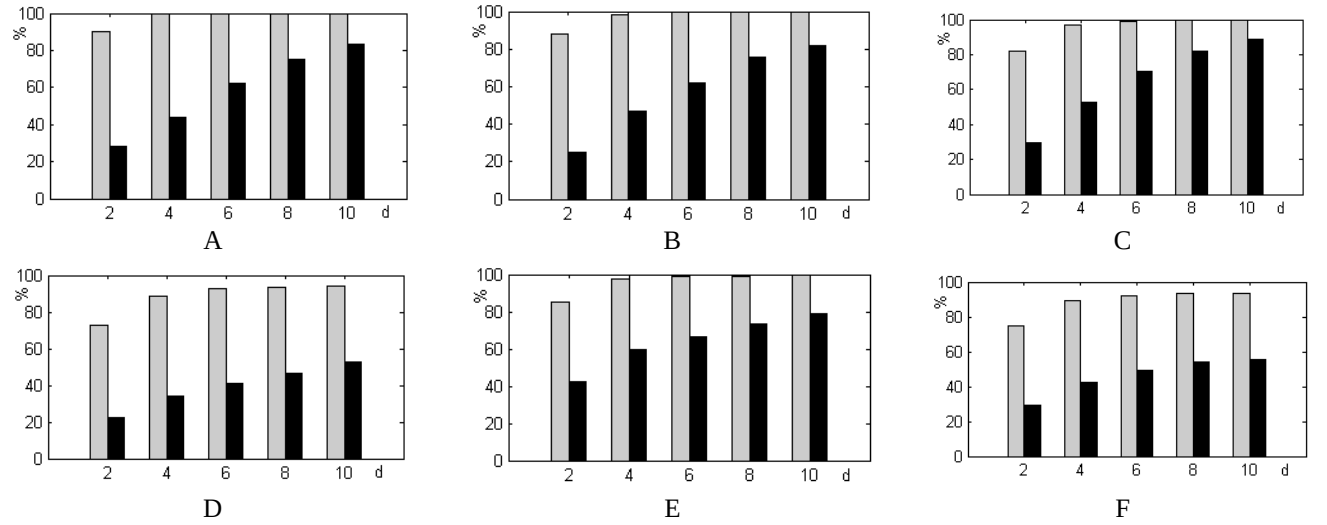

Fig. 8. The results of the boundary extracted. A - the noise free images (radiologist1-radiologist2), B - the cluttered images (radiologist1-radiologist2), C - the noise free images (radiologist1-program), D - the cluttered images (radiologist1-program), E - the noise free images (radiologist2-program), F - the cluttered images (radiologist2-program). The gray bars correspond to the lower boundary, the black bars correspond to the upper boundary.

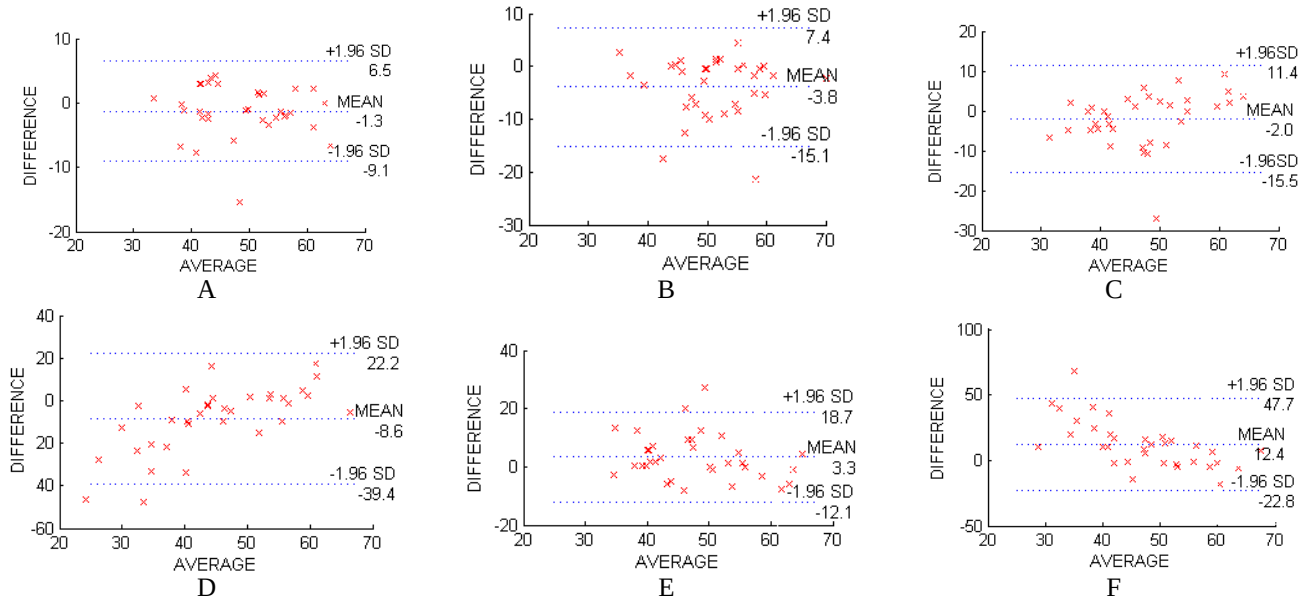

Fig. 9. The cortical width measurement described by the Bland-Atman plot (SD is the standard deviation of the differences, MEAN is the mean value of the differences).A - the noise free images (radiologist1-radiologist2), B - the cluttered images (radiologist1-radiologist2), C - the noise free images (radiologist1-program), D - the cluttered images (radiologist1-program), E - the noise free images (radiologist2-program), F - the cluttered images (radiologist2-program).

VII. ACKNOWLEDGMENTS

The authors would like to thank Marta Dyszkiewicz (University of Medical Sciences, Poznan, Section of Dental Radiology) as the second maxillofacial radiologist, who drew the upper and lower boundaries of the mandible.

VIII. LITERATURE

[1] M. Van der Klift , H.A. Pols, JM Gelenijse, D.A.M, Van der Kuip, A. Hofman, C.E.D.H De Laet, "Bone mineral density and mortality in elderly men and women," *Bone*, 30, pp. 643-651, 2002.

[2] K. Horner, H. Devlin, C.W. Alsop, I.M. Hodgkinson, J.E Adams, "Mandibular bone mineral density as a predictor of skeletal osteoporosis," *British Journal of Radiology*, 69, pp. 1019-1025, 1996.

[3] K. Horner, H. Devlin, L. Harvey "Detecting patients with low skeletal bone mass," *Journal of Dentistry*, 30, pp. 171-175, 2002.

[4] L. Choel, F. Duboeuf, D. Bourgeois, A. Briguet, M. Lissac, "Trabecular alveolar bone in the human mandible: a dual- energy x-ray absorptiometry study," *Oral Surgery, Oral Medicine, Oral Pathology, Oral Radiology, and Endodontics*, 95, pp. 364-370, 2003.

[5] W.G.M. Geraets, J.G.C. Verheij, P.F. van der Stelt, K. Horner,C. Lindh, K. Nicopoulou-Karayianni, R. Jacobs, E.J. Harrison, J.E. Adams, H. Devlin "Prediction of bone mineral density with dental radiographs," *Bone*, 40, pp. 1217-1221, 2007

[6] P. D. Allen, J. Graham, D. J. J. Farnell, E. J. Harrison, R. Jacobs, K. Nicopolou-Karayianni, C. Lindh, P. F. van der Stelt, K. Horner, H. Devlin, "Detecting Reduced Bone Mineral Density From Dental Radiographs Using Statistical Shape Models," *IEEE Transaction on Information Technology in Biomedicine*, 6, pp. 601-610, 2007.

[7] A. Z. Arifin, A. Asano, A. Taguchi, T. Nakamoto, M. Ohtsuka, M. Tsuda, Y. Kudo, K. Tanimoto, "Computer-aided system for measuring the mandibular cortical width on dental panoramic radiographs in identifying postmenopausal women with low bone mineral density," *Osteoporosis International*, 17, pp. 753-759, 2006.

[8] K. Karayianni, K. Horner, A. Mitsea, L. Berkas, M. Mastoris, R. Jacobs, C. Lindh, P.F. van der Stelt, E. Harrison, J.E. Adams, S. Pavitt, H. Devlin, "Accuracy in osteoporosis diagnosis of a combination of mandibular cortical width measurement on dental panoramic radiographs and a clinical risk index (OSIRIS): The OSTEODENT project," *Bone*, 40, pp. 223–229, 2007.

[9] E. N. Mortensen, W. A. Barrett, "Interactive Segmentation with Intelligent Scissors," *Graphical Models and Image Processing*, 60, pp. 349–384, 1998.

[10] A.Z. Arifin, , A. Asano, A. Taguchi, T. Nakamoto, M. Ohtsuka, K. Tanimoto, "Computer-aided system for measuring the mandibular cortical width on panoramic radiographs in osteoporosis diagnosis" , *Progress in Biomedical Optics and Imaging - Proceedings of SPIE*, 5747, pp. 813-821, 2005.